

A Space-Time Continuous Galerkin Finite Element Method for Linear Schrödinger Equations

Marco Zank

Institut für Analysis und Scientific Computing, TU Wien, Vienna, Austria
marco.zank@tuwien.ac.at

Abstract

We introduce a space-time finite element method for the linear time-dependent Schrödinger equation with Dirichlet conditions in a bounded Lipschitz domain. The proposed discretization scheme is based on a space-time variational formulation of the time-dependent Schrödinger equation. In particular, the space-time method is conforming and is of Galerkin-type, i.e., trial and test spaces are equal. We consider a tensor-product approach with respect to time and space, using piecewise polynomial, continuous trial and test functions. In this case, we state the global linear system and efficient direct space-time solvers based on exploiting the Kronecker structure of the global system matrix. This leads to the Bartels–Stewart method and the fast diagonalization method. Both methods result in solving a sequence of spatial subproblems. In particular, the fast diagonalization method allows for solving the spatial subproblems in parallel, i.e., a time parallelization is possible. Numerical examples for a two-dimensional spatial domain illustrate convergence in space-time norms and show the potential of the proposed solvers.

Keywords: linear time-dependent Schrödinger equation · space-time method · direct solver · time parallelization

1 Introduction

The Schrödinger equation is the central governing equation in quantum mechanics, where its solution, the wave function, is usually complex-valued and yields the time evolution of the state in quantum mechanics. Moreover, in several physical fields, the Schrödinger equation plays a major role. Classical approaches for computing approximate solutions for Schrödinger equations separate the temporal and spatial directions. In particular, time-stepping schemes are applied in connection with different spatial discretizations, e.g., finite difference methods, finite element methods or spectral methods. We refer to the overview in the review article [9]. An alternative is an approach via space-time methods, where the temporal variable t is just another spatial variable. Recently, space-time methods for the linear Schrödinger equation have been introduced. In particular, nonconforming approaches of discontinuous Galerkin-type are considered in [4] and [6]. In [2], a least squares approach based on [4] is considered, whereas [7] relies on an ultraweak variational formulation. However, these approaches in [2] and [7] require H^2 conformity, which could lead to a delicate construction of the approximation spaces.

In this work, we introduce a space-time finite element method for the time-dependent Schrödinger equation, which only requires H^1 conformity. We apply a tensor-product approach using piecewise polynomial, continuous trial and test functions. We state the resulting global linear system. Further, we investigate efficient direct space-time solvers, including time parallelization, which are based on the Bartels–Stewart method [1] or on the fast diagonalization method [10]. The model problem is the nondimensionalized time-dependent Schrödinger equation with Dirichlet conditions to find the wave function $\psi: \bar{\Omega} \times [0, T] \rightarrow \mathbb{C}$ such that

$$\left. \begin{aligned} i\partial_t\psi(x, t) - \Delta_x\psi(x, t) &= f(x, t) && \text{for } (x, t) \in Q = \Omega \times (0, T), \\ \psi(x, t) &= 0 && \text{for } (x, t) \in \partial\Omega \times [0, T], \\ \psi(x, 0) &= \psi_0(x) && \text{for } x \in \Omega, \end{aligned} \right\} \quad (1)$$

where $f: \Omega \times (0, T) \rightarrow \mathbb{C}$ is a given right-hand side, and $\psi_0: \Omega \rightarrow \mathbb{C}$ is a given initial condition. Further, $\Omega \subset \mathbb{R}^d$, $d \in \mathbb{N}$, is a bounded Lipschitz domain, which is an interval $\Omega = (0, L)$ for $d = 1$, polygonal for $d = 2$, or polyhedral for $d = 3$, and $T > 0$ is the terminal time.

The rest of the paper is organized as follows: In Section 2, the used function spaces and the unique solvability of the Schrödinger equation are considered. Section 3 is devoted to the introduction of the space-time finite element method and space-time solvers. In Section 4, we present numerical examples in a two-dimensional spatial domain. Finally, we draw some conclusions in Section 5.

2 Functional Framework

In this section, we introduce function spaces and state unique solvability for the time-dependent Schrödinger equation (1). For this purpose, we define the solution space

$$W(Q) = \{u \in L^2(0, T; H_0^1(\Omega)) : \partial_t u \in L^2(0, T; [H_0^1(\Omega)]^*)\}.$$

As $W(Q) \subset C([0, T]; L^2(\Omega))$, we introduce the subspace

$$W_0(Q) = \{u \in W(Q) : u(\cdot, 0) = 0\}.$$

Here, all spaces are complex vector spaces. In particular, the usual Lebesgue space $L^2(D)$ consists of complex-valued functions $u: D \rightarrow \mathbb{C}$ and is endowed with the inner product

$$\langle u, v \rangle_{L^2(D)} = \int_D u(x) \overline{v(x)} dx,$$

where $D \subset \mathbb{R}^m$, $m \in \mathbb{N}$, is a bounded Lipschitz domain. Analogously, we consider a vector-valued version $L^2(D)^m$ and the extension to Bochner spaces $L^2(0, T; X)$ for a complex Hilbert space X . Moreover, the Sobolev space $H_0^1(D)$ consists of complex-valued functions, which are zero on the boundary ∂D , and we equip $H_0^1(D)$ with the inner product $\langle u, v \rangle_{H_0^1(D)} = \langle \nabla_x u, \nabla_x v \rangle_{L^2(D)^m}$, inducing a norm due to the Poincaré inequality. The antidual $[H_0^1(D)]^*$ is the space of conjugate linear continuous functionals from $H_0^1(D)$ to \mathbb{C} , where $\langle \cdot, \cdot \rangle_D$ extends continuously the $L^2(D)$ inner product to functionals. Last, the space $C([0, T]; X)$ contains all continuous functions $u: [0, T] \rightarrow X$ for a complex Hilbert space X . With this notation, we state the unique solvability of the time-dependent Schrödinger equation (1).

Theorem 1. *Let the given right-hand side $f \in L^2(Q)$ satisfy the condition*

$$\partial_t f \in L^2(0, T; [H_0^1(\Omega)]^*)$$

and let the given initial data $\psi_0 \in H_0^1(\Omega)$. Then, a unique solution $\psi \in W(Q)$ to the time-dependent Schrödinger equation (1) exists such that the regularity results

$$\psi \in C([0, T]; H_0^1(\Omega)) \quad \text{and} \quad \partial_t \psi \in C([0, T]; [H_0^1(\Omega)]^*)$$

hold true.

Proof. The unique solvability is proven in [3, Theorem 1, Section 7 in Chapter XVIII]. The regularity results are given in [3, Remark 3, Section 7 in Chapter XVIII]. \square

3 Space-Time Finite Element Method

In this section, we design a space-time finite element method for the time-dependent Schrödinger equation (1), which are based on a space-time variational setting stated first. The solution $\psi \in W(Q)$ of Theorem 1 satisfies the space-time variational formulation to find $\psi \in W(Q)$ such that $\psi(\cdot, 0) = \psi_0$ and

$$\forall v \in L^2(0, T; H_0^1(\Omega)) : \quad a(\psi, v) = \langle f, v \rangle_{L^2(Q)} \quad (2)$$

with the sesquilinear form $a(\cdot, \cdot) : W(Q) \times L^2(0, T; H_0^1(\Omega)) \rightarrow \mathbb{C}$,

$$a(u, v) = i \langle \partial_t u, v \rangle_Q + \langle \nabla_x u, \nabla_x v \rangle_{L^2(Q)^d}.$$

Further, we introduce the function

$$\widehat{\psi}(x, t) = \psi(x, t) - \psi_0(x) \quad \text{for } (x, t) \in Q,$$

which satisfies $\widehat{\psi} \in W_0(Q)$. Plugging this into the variational formulation (2) yields the space-time variational formulation to find $\widehat{\psi} \in W_0(Q)$ such that

$$\forall v \in L^2(0, T; H_0^1(\Omega)) : \quad a(\widehat{\psi}, v) = \langle f, v \rangle_{L^2(Q)} - a(\psi_0, v).$$

Next, we introduce the approximation spaces used for the space-time finite element method. For this purpose, we decompose the spatial domain Ω by $\overline{\Omega} = \bigcup_{\ell=1}^{N_x} \overline{\omega}_\ell$ with $N_x \in \mathbb{N}$ spatial elements $\omega_\ell \subset \mathbb{R}^d$, where we assume that the spatial mesh

$$\mathcal{T} = \{\omega_\ell\}_{\ell=1}^{N_x}$$

is admissible. In the following, a shape-regular sequence $(\mathcal{T}_\nu)_{\nu \in \mathbb{N}}$ of decompositions of Ω is considered, which, for simplicity, consists of intervals for $d = 1$, triangles for $d = 2$, and tetrahedra for $d = 3$ as elements ω_ℓ . The temporal mesh is given by the vertices

$$0 = t_0 < t_1 < \dots < t_{N_t} = T$$

for $N_t \in \mathbb{N}$ elements $(t_{\ell-1}, t_\ell) \subset \mathbb{R}$. We denote by h_x and h_t the maximal mesh size with respect to space and time, respectively. To the temporal mesh and the spatial mesh \mathcal{T}_ν , we relate the space-time finite element space

$$Q_h^p(Q) = S_{h_x}^p(\Omega) \otimes S_{h_t}^p(0, T)$$

for a given polynomial degree $p \in \mathbb{N}$. Here, $S_{h_x}^p(\Omega)$ is the space of piecewise polynomial, continuous and complex-valued functions on intervals for $d = 1$, or triangles for $d = 2$, or tetrahedra for $d = 3$ such that $v|_{\bar{\omega}}$ is a polynomial function of degree p for all elements $\omega \in \mathcal{T}_\nu$, where $v \in S_{h_x}^p(\Omega)$. Analogously, we define $S_{h_t}^p(0, T)$ as the space of piecewise polynomial, continuous and complex-valued functions. Last, we introduce the subspace $Q_{h,0}^p(Q) = Q_h^p(Q) \cap W_0(Q)$ of complex-valued functions, which satisfy the homogeneous initial and boundary conditions. With this, we consider the conforming space-time finite element method to find $\psi_h \in Q_{h,0}^p(Q)$ such that

$$\forall v_h \in Q_{h,0}^p(Q) : \quad a(\widehat{\psi}_h, v_h) = \langle f, v_h \rangle_{L^2(Q)} - a(\psi_0, v_h). \quad (3)$$

Finally, we define the approximation $\psi \approx \psi_h$ by

$$\psi_h(x, t) = \widehat{\psi}_h(x, t) + \psi_0(x) \quad \text{for } (x, t) \in Q.$$

The numerical analysis of the space-time finite element method (3) is not in the scope of this work and will be investigated in future work. Anyway, in this work, we focus on space-time solvers for the space-time finite element method (3). For this purpose, we state the resulting global linear system

$$(iB_t \otimes M_x + M_t \otimes A_x)\boldsymbol{\psi} = \mathbf{f}. \quad (4)$$

Here, the real-valued, spatial matrices $M_x, A_x \in \mathbb{R}^{n_x \times n_x}$ are defined by

$$M_x[k, j] = \int_{\Omega} \phi_j(x)\phi_k(x)dx \quad \text{and} \quad A_x[k, j] = \int_{\Omega} \nabla_x \phi_j(x) \cdot \nabla_x \phi_k(x)dx \quad (5)$$

for $k, j = 1, \dots, n_x$ with real-valued basis functions $\phi_k: \bar{\Omega} \rightarrow \mathbb{R}$. The real-valued, temporal matrices $M_t, B_t \in \mathbb{R}^{n_t \times n_t}$ are

$$M_t[k, j] = \int_0^T \varphi_j(t)\varphi_k(t)dt \quad \text{and} \quad B_t[k, j] = \int_0^T \partial_t \varphi_j(t)\varphi_k(t)dt \quad (6)$$

for $k, j = 1, \dots, n_t$ with real-valued basis functions $\varphi_k: [0, T] \rightarrow \mathbb{R}$. The right-hand side $\mathbf{f} \in \mathbb{C}^{n_x \cdot n_t}$ of the linear system (4) is given analogously. Note that the number of spatial degrees of freedom is n_x , whereas the number of temporal degrees of freedom is n_t , which leads to the total number of degrees of freedom $n = n_x \cdot n_t$.

Next, we state efficient space-time solvers for the global linear system (4). To develop such space-time solvers, which exploit the Kronecker structure of the global linear system (4), we assume the temporal decomposition

$$(iB_t)^{-1}M_t = X_t S_t X_t^{-1}.$$

Here, the matrix X_t is regular, and the matrix $S_t \in \mathbb{C}^{n_t \times n_t}$ is regular and upper triangular, where X_t, S_t have to be specified. Further, we set

$$Y_t = X_t^{-1}(iB_t)^{-1}.$$

With these representations, the solution $\boldsymbol{\psi} \in \mathbb{C}^{n_x \cdot n_t}$ of the global linear system (4) is given by

$$\boldsymbol{\psi} = (X_t \otimes I_{n_x})(I_{n_t} \otimes M_x + S_t \otimes A_x)^{-1}(Y_t \otimes I_{n_x})\mathbf{f},$$

see [5, Section 3.2] and [8, Eq. (4.2)], where $I_{n_t} \in \mathbb{R}^{n_t \times n_t}$, $I_{n_x} \in \mathbb{R}^{n_x \times n_x}$ are identity matrices. This leads to the following Kronecker product solver, see [5, Algorithm 1], [8, Algorithm 4.2] for the real-valued case:

1. Compute the matrices X_t, S_t of the decomposition $(iB_t)^{-1}M_t = X_t S_t X_t^{-1}$.
2. Calculate $\mathbf{g} = (\mathbf{g}_1, \dots, \mathbf{g}_{n_t})^\top = (Y_t \otimes I_{n_x})\mathbf{f}$ with the vectors $\mathbf{g}_\ell \in \mathbb{C}^{n_x}$.
3. For $\ell = n_t, n_t - 1, \dots, 1$, solve the spatial problems

$$(M_x + S_t[\ell, \ell]A_x)\mathbf{w}_\ell = \mathbf{g}_\ell - \sum_{k=\ell+1}^{n_t} S_t[\ell, k]A_x\mathbf{w}_k \quad (7)$$

for $\mathbf{w}_\ell \in \mathbb{C}^{n_x}$, where $\sum_{k=n_t+1}^{n_t}(\cdot) = 0$.

4. Compute the solution $\boldsymbol{\psi} \in \mathbb{C}^{n_x \cdot n_t}$ by $\boldsymbol{\psi} = (X_t \otimes I_{n_x})\mathbf{w}$.

Note that steps 2 and 4 consists of few matrix multiplications, which are parallelizable and can be written as highly efficient operations, see [8, Subsection 4.3.1, Subsection 4.4.1]. In the case that $n_t \ll n_x$, the most expensive part is step 3, i.e., solving n_t spatial subproblems of size n_x . This can be done by an iterative solver [5] or by sparse direct solvers [8]. The latter is considered in this work.

Finally, we state two choices for the complex matrices X_t, S_t of the decomposition

$$(iB_t)^{-1}M_t = X_t S_t X_t^{-1}$$

in step 1 of the proposed solver:

1. Bartels–Stewart method [1]: The first choice is the Schur decomposition leading to a unitary matrix X_t and an upper triangular matrix S_t with the eigenvalues of $(iB_t)^{-1}M_t$ on the diagonal of S_t .
2. Fast diagonalization method [10]: The second choice is the eigenvalue decomposition resulting in the matrix X_t consisting of eigenvectors of the matrix $(iB_t)^{-1}M_t$ and the diagonal matrix S_t , where the diagonal is composed of the eigenvalues of $(iB_t)^{-1}M_t$. Here, we have to assume that the matrix $(iB_t)^{-1}M_t$ is diagonalizable. This is the case for a uniform temporal mesh size, see Table 2 in Section 4 and [5, Section 3.2]. However, for a complete analysis of these eigenvalues, we refer to future work. Anyway, the sum on the right side of the spatial linear systems (7) is zero. Thus, the spatial linear systems (7) can be solved in parallel, i.e., a time parallelization is possible.

4 Numerical Experiments

In this section, we state numerical examples, which show the potential of the space-time finite element method (3) proposed in this work. We consider the unit square $\Omega = (0, 1) \times (0, 1) \subset \mathbb{R}^2$ as spatial domain and $T = 5$. The initial spatial mesh is stated in Fig. 1, where we apply a uniform refinement strategy such that we have $N_x = 2048 \cdot 4^J$ spatial elements for the refinement levels $J = 0, \dots, 4$. The uniform temporal mesh is given by

$$t_\ell = \frac{T\ell}{N_t} \quad \text{for } \ell = 0, \dots, N_t \quad (8)$$

with $N_t = 64 \cdot 2^J$ for $J = 0, \dots, 4$, see Fig. 1. The wave function $\psi: \overline{Q} \rightarrow \mathbb{C}$,

$$\psi(x_1, x_2, t) = e^{it} \sin(\pi x_1) \sin(\pi x_2) \sin(tx_1 x_2), \quad (x_1, x_2, t) \in \overline{Q},$$

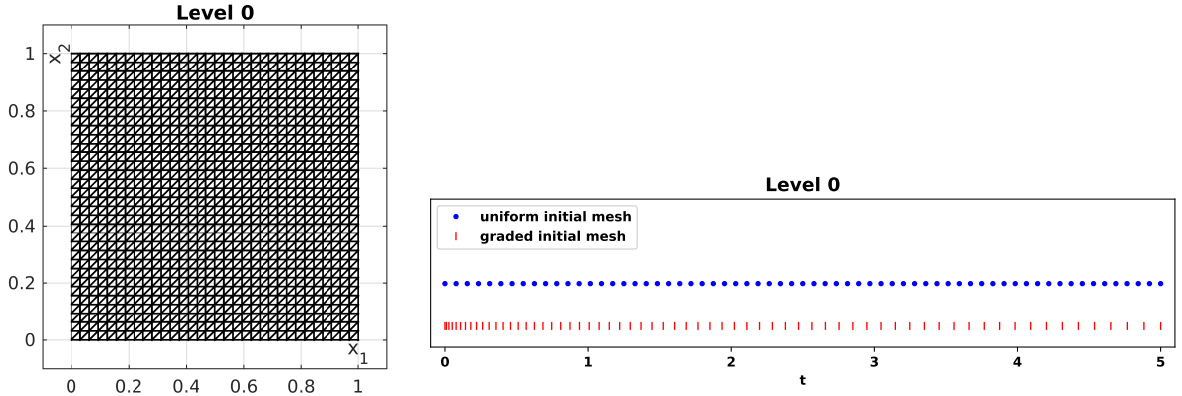


Fig. 1: Initial spatial mesh for $\Omega = (0, 1) \times (0, 1)$ and initial temporal meshes for $T = 5$.

Table 1: Results of the finite element method (3) with $p = 1$, the temporal mesh (8) for $T = 5$ and the initial spatial mesh in Fig. 1 using the Bartels–Stewart method.

| n | h_x | h_t | $\ \psi - \psi_h\ _{L^2(Q)}$ | eoc | $ \psi - \psi_h _{H^1(Q)}$ | eoc | Solve in s |
|-----------|---------|---------|------------------------------|-----|----------------------------|-----|------------|
| 61504 | 2.2e-02 | 7.8e-02 | 3.2e-03 | - | 2.4e-01 | - | 0.3 |
| 508032 | 1.1e-02 | 3.9e-02 | 8.1e-04 | 1.9 | 1.2e-01 | 1.0 | 3.1 |
| 4129024 | 5.5e-03 | 2.0e-02 | 2.0e-04 | 2.0 | 6.0e-02 | 1.0 | 30.9 |
| 33292800 | 2.8e-03 | 9.8e-03 | 5.1e-05 | 2.0 | 3.0e-02 | 1.0 | 405.4 |
| 267387904 | 1.4e-03 | 4.9e-03 | 1.3e-05 | 2.0 | 1.5e-02 | 1.0 | 4869.8 |

is considered as exact solution to the time-dependent Schrödinger equation (1) with the corresponding right-hand side f and the initial condition $\psi(x_1, x_2, 0) = \psi_0(x_1, x_2) = 0$. In other words, we have that $\hat{\psi} = \psi$ and $\hat{\psi}_h = \psi_h$. We consider the polynomial degree $p = 1$, i.e., the approximate solution $\psi_h \in Q_{h,0}^p(Q)$ given by the space-time finite element method (3) is a piecewise multilinear function. We choose the usual nodal basis functions, i.e., the hat functions with respect to time, to compute analytically the matrices M_x, A_x in (5) and the matrices M_t, B_t in (6). To calculate the vector of the right-hand side \mathbf{f} of the linear system (4), we apply high-order numerical integration. The numerical experiments were performed in MATLAB R2022a using internal MATLAB routines on a PC with two Intel Xeon CPUs E5-2687W v4 @ 3.00GHz, having 512 GB memory and 24 cores. In particular, we use the MATLAB routine `mldivide` (backslash operator) for solving the spatial problems (7) by a sparse direct solver.

In Table 1, we state the errors in space-time norms $\|\cdot\|_{L^2(Q)}$ and

$$|\cdot|_{H^1(Q)} = \left(\|\partial_t(\cdot)\|_{L^2(Q)}^2 + \|\nabla_x(\cdot)\|_{L^2(Q)^d}^2 \right)^{1/2}$$

and the solving time in seconds s , which includes all steps of the Bartels–Stewart method but excludes the assembling time of the matrices M_x, A_x, M_t, B_t and the vector \mathbf{f} . Here, we use a uniform refinement strategy for the spatial and temporal meshes, i.e., we quadruple the number of spatial elements N_x and double the number of temporal elements N_t . Thus, the total number of degrees of freedom $n = n_x \cdot n_t$ grows by a factor 8. We observe second-order convergence in $\|\cdot\|_{L^2(Q)}$ and first-order convergence in $|\cdot|_{H^1(Q)}$.

In Table 2, we consider the same situation as in Table 1. However, we apply the fast

Table 2: Results of the finite element method (3) with $p = 1$, the temporal mesh (8) for $T = 5$ and the initial spatial mesh in Fig. 1 using the fast diagonalization method.

| n | h_x | h_t | $\ \psi - \psi_h\ _{L^2(Q)}$ | eoc | $ \psi - \psi_h _{H^1(Q)}$ | eoc | Solve in s | $\kappa_2(X_t)$ |
|-----------|---------|---------|------------------------------|-----|----------------------------|-----|------------|-----------------|
| 61504 | 2.2e-02 | 7.8e-02 | 3.2e-03 | - | 2.4e-01 | - | 0.1 | 2.3e+02 |
| 508032 | 1.1e-02 | 3.9e-02 | 8.1e-04 | 1.9 | 1.2e-01 | 1.0 | 0.3 | 7.0e+02 |
| 4129024 | 5.5e-03 | 2.0e-02 | 2.0e-04 | 2.0 | 6.0e-02 | 1.0 | 2.3 | 2.2e+03 |
| 33292800 | 2.8e-03 | 9.8e-03 | 5.1e-05 | 2.0 | 3.0e-02 | 1.0 | 20.5 | 7.1e+03 |
| 267387904 | 1.4e-03 | 4.9e-03 | 1.3e-05 | 2.0 | 1.5e-02 | 1.0 | 248.8 | 2.4e+04 |

Table 3: Results of the finite element method (3) with $p = 1$, graded initial mesh in t for $T = 5$ and the initial spatial mesh in Fig. 1 using the fast diagonalization method.

| n | h_x | h_t | $\ \psi - \psi_h\ _{L^2(Q)}$ | eoc | $ \psi - \psi_h _{H^1(Q)}$ | eoc | Solve in s | $\kappa_2(X_t)$ |
|-----------|---------|---------|------------------------------|-----|----------------------------|-----|------------|-----------------|
| 61504 | 2.2e-02 | 1.2e-01 | 3.2e-03 | - | 2.4e-01 | - | 0.1 | 1.1e+02 |
| 508032 | 1.1e-02 | 5.8e-02 | 8.4e-04 | 1.9 | 1.2e-01 | 1.0 | 0.3 | 3.6e+02 |
| 4129024 | 5.5e-03 | 2.9e-02 | 2.1e-04 | 2.0 | 6.1e-02 | 1.0 | 2.1 | 1.1e+03 |
| 33292800 | 2.8e-03 | 1.5e-02 | 5.4e-05 | 2.0 | 3.0e-02 | 1.0 | 20.7 | 3.6e+03 |
| 267387904 | 1.4e-03 | 7.3e-03 | 1.3e-05 | 2.0 | 1.5e-02 | 1.0 | 246.6 | 1.2e+04 |

diagonalization method for solving the global linear system (4). Moreover, we solve the spatial linear systems (7) in parallel using 24 cores. Thus, there is no parallelization for the direct solver `mldivide` (backslash operator) possible. We observe the identical errors as for the Bartels–Stewart method in Table 1. Comparing the solving times in Table 2 and Table 1 yields that the solving time is drastically decreased by applying the fast diagonalization method. In the last column of Table 2, we state the spectral condition number $\kappa_2(X_t)$ of the transformation matrix X_t related to the eigenvectors of the matrix $(iB_t)^{-1}M_t$. We report that $\kappa_2(X_t)$ does not depend on the terminal time T , i.e., $\kappa_2(X_t)$ depends solely on the number n_t of degrees of freedom in the case of a uniform mesh size h_t . Further, we observe that the spectral condition number $\kappa_2(X_t)$ does not grow exponentially with respect to n_t . In other words, the fast diagonalization method is applicable also for a high number of temporal degrees of freedom.

Last, in Table 3, we consider the situation as in Table 2, except that we replace the initial mesh in t with the graded mesh

$$\{t_\ell = T \left(\frac{\ell}{64}\right)^q : \ell = 0, \dots, 64\}$$

with $q = 1.5$, see Fig. 1. This initial mesh is refined uniformly when increasing the refinement level. Note that for these temporal meshes, $h_t \approx 12 \cdot h_{t,\min}$ holds with $h_{t,\min} = \min_\ell |t_\ell - t_{\ell-1}|$. We report that the Bartels–Stewart method and the fast diagonalization method lead to identical errors. In particular, the fast diagonalization method is also applicable for these non-uniform temporal meshes.

5 Conclusions

In this work, we introduced an H^1 conforming space-time finite element method for the linear time-dependent Schrödinger equation, using piecewise polynomial, continuous trial and test functions. Moreover, we stated efficient direct space-time solvers leading to the Bartels–Stewart method and the fast diagonalization method. The latter allows for time paralleliza-

tion. We presented numerical examples for a two-dimensional spatial domain, which show the potential of the proposed methods.

Acknowledgments

This research was funded in part by the Austrian Science Fund (FWF) [10.55776/P36150].

Declarations

The author has no competing interests to declare that are relevant to the content of this article.

References

- [1] Bartels, R.H., Stewart, G.W.: Algorithm 432: Solution of the matrix equation $AX + XB = C$. *Commun. ACM* **15**, 820–826 (1972)
- [2] Bressan, A., Kushova, A., Sangalli, G., Tani, M.: Space-time least squares approximation for Schrödinger equation and efficient solver (arXiv:2311.18461) (2023)
- [3] Dautray, R., Lions, J.L.: *Mathematical analysis and numerical methods for science and technology. Vol. 5: Evolution problems I*. Springer-Verlag, Berlin (1992)
- [4] Demkowicz, L., Gopalakrishnan, J., Nagaraj, S., Sepúlveda, P.: A spacetime DPG method for the Schrödinger equation. *SIAM J. Numer. Anal.* **55**(4), 1740–1759 (2017)
- [5] Foltyn, L., Lukáš, D., Zank, M.: Robust PRESB Preconditioning of a 3-Dimensional Space-Time Finite Element Method for Parabolic Problems. *Comput. Methods Appl. Math.* **24**(2), 439–451 (2024)
- [6] Gómez, S., Moiola, A.: A space-time DG method for the Schrödinger equation with variable potential. *Adv. Comput. Math.* **50**(2), 34 (2024)
- [7] Hain, S., Urban, K.: An ultra-weak space-time variational formulation for the Schrödinger equation. *J. Complexity* **85**, 22 (2024)
- [8] Langer, U., Zank, M.: Efficient direct space-time finite element solvers for parabolic initial-boundary value problems in anisotropic Sobolev spaces. *SIAM J. Sci. Comput.* **43**(4), A2714–A2736 (2021)
- [9] Lasser, C., Lubich, C.: Computing quantum dynamics in the semiclassical regime. *Acta Numer.* **29**, 229–401 (2020)
- [10] Lynch, R., Rice, J.R., Thomas, D.H.: Direct solution of partial difference equations by tensor product methods. *Numer. Math.* **6**, 185–199 (1964)